

Tandem Effect of Atomically Isolated Copper–Nitrogen Sites and Copper Clusters Enhances CO₂ Electroreduction to Ethylene

Ying Zhang,*^{a,1} Jianing Gui,^{a,1} Dan Wang,^a Junjun Mao,^a Chenchen Zhang^a and Fengwang Li*^b

a. Key Laboratory of Synthetic and Biological Colloids Ministry of Education, School of Chemical and Material Engineering, Jiangnan University, Wuxi 214122, China

b. School of Chemical and Biomolecular Engineering, the University of Sydney, NSW 2006, Australia.

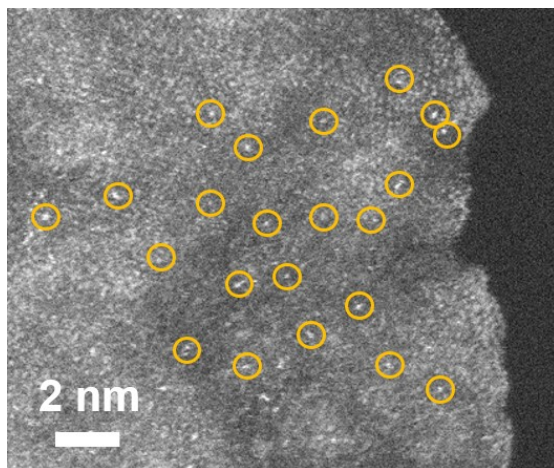


Figure S1. STEM image of PDI-Cu

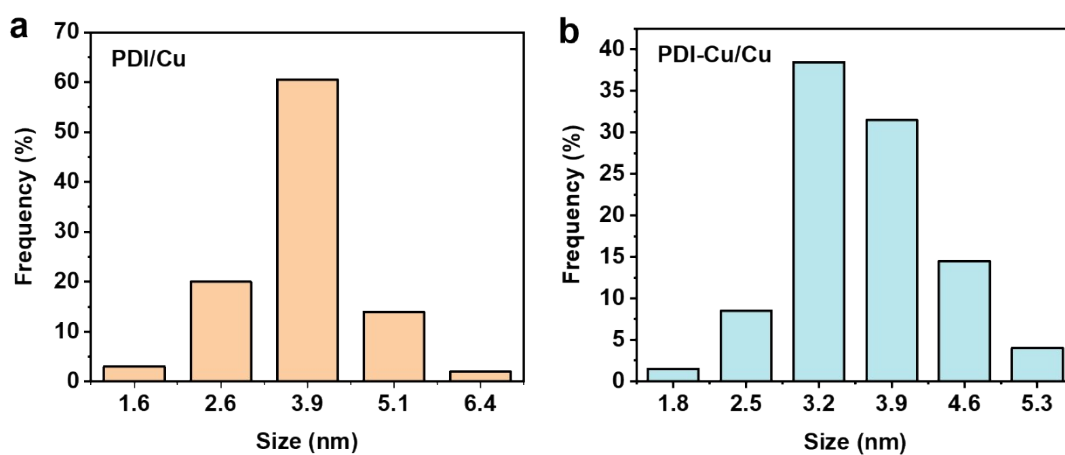


Figure S2. size distribution of Cu clusters on (a) PDI/Cu and (b) PDI-Cu/Cu.

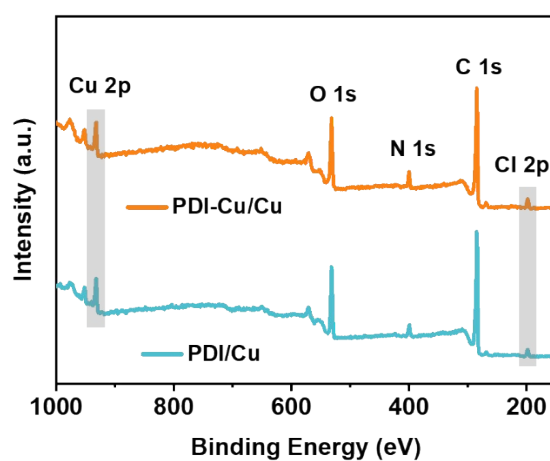


Figure S3. The full XPS survey spectra.

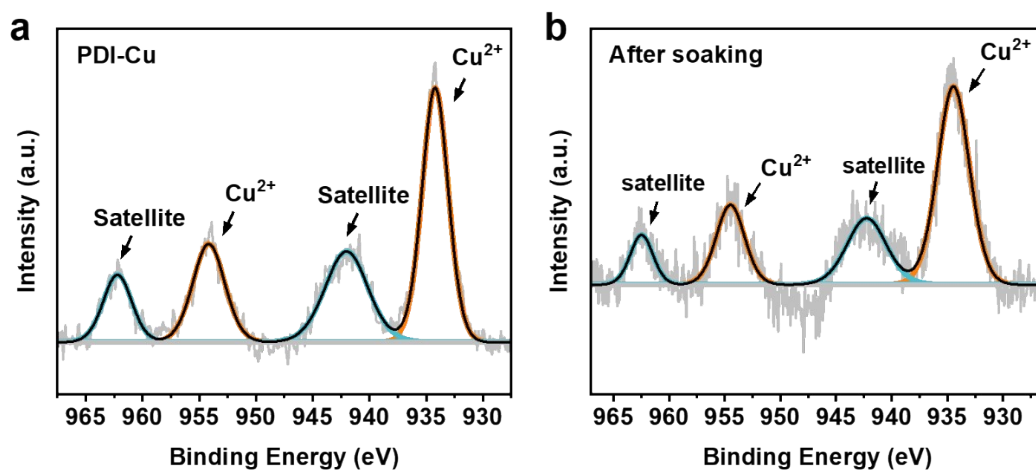


Figure S4. Cu 2p XPS spectra of (a) PDI-Cu and (b) PDI-Cu after soaking *L*-ascorbic acid.

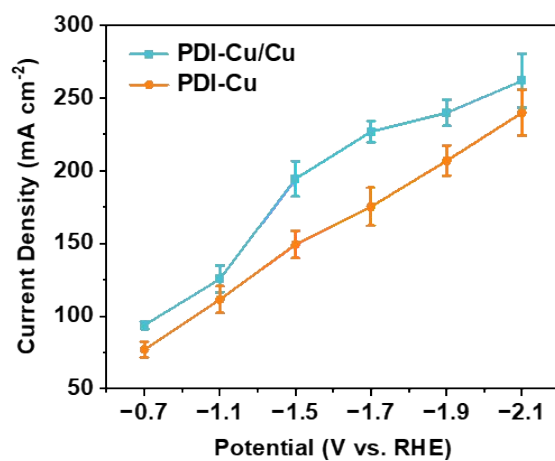


Figure S5. Total current densities of PDI-Cu/Cu and PDI/Cu.

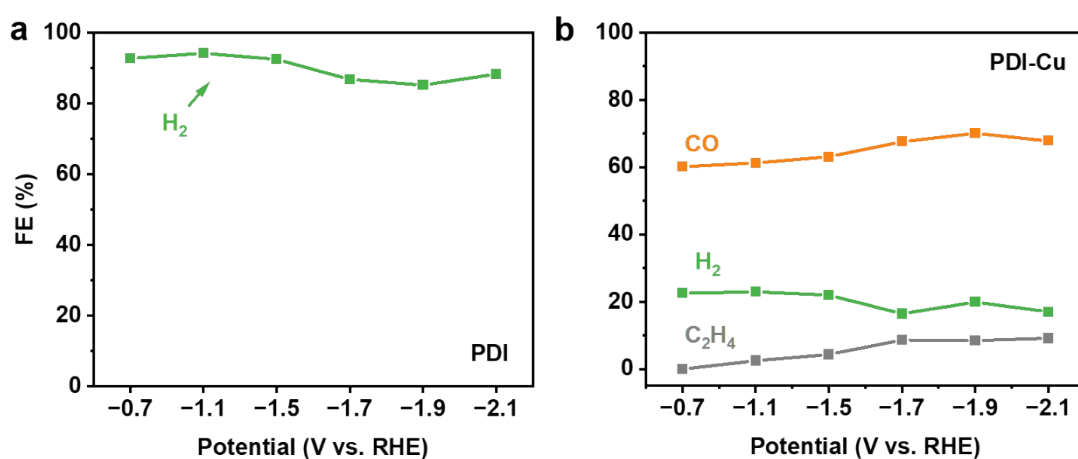


Figure S6. FEs of different products for (a) PDI and (b) PDI-Cu.

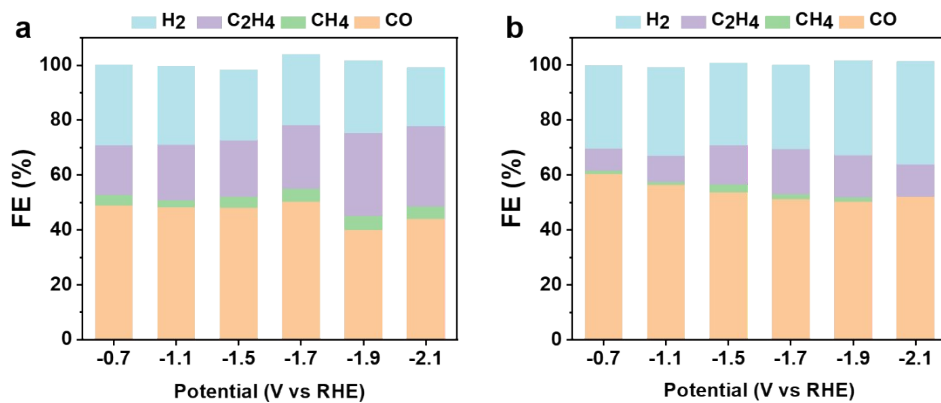


Figure S7. FEs of CO₂RR products at different applied potentials (V vs. RHE) catalyzed by (a) PDI-Cu/Cu and (b) PDI/Cu.

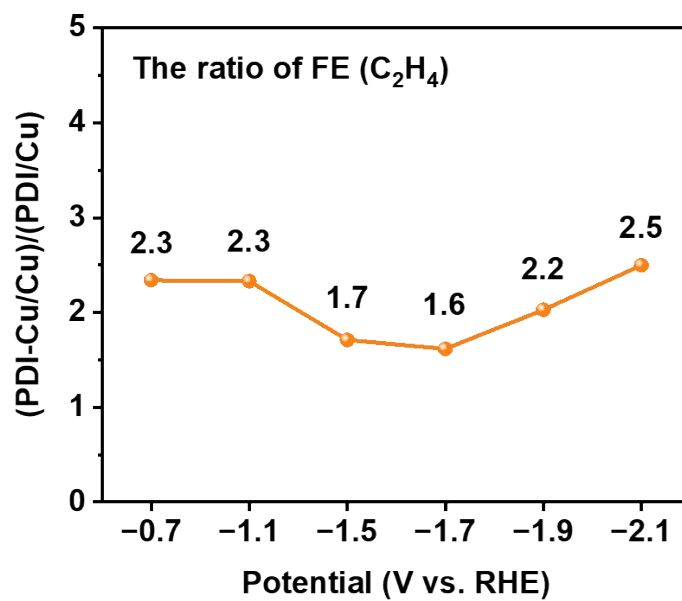


Figure S8. The FE (C₂H₄) ratio of PDI-Cu/Cu to PDI/Cu.

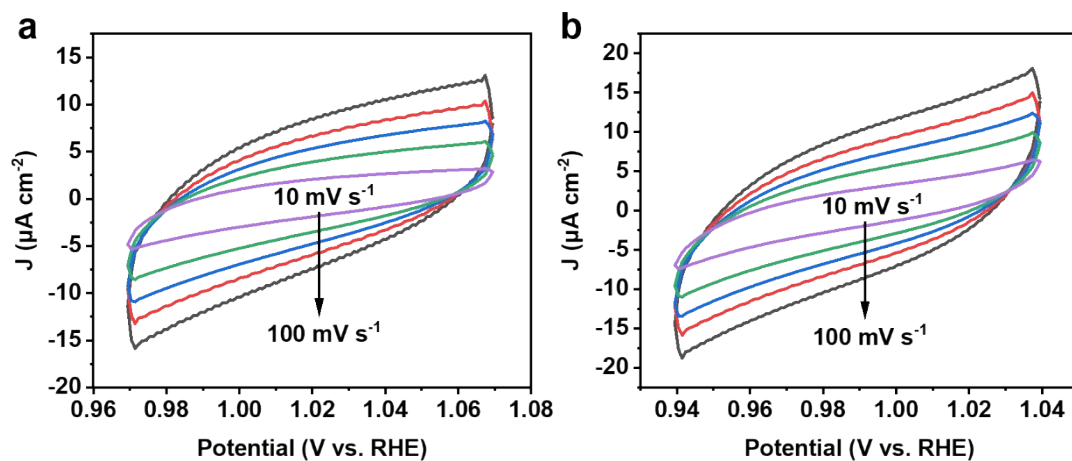


Figure S9. Typical cyclic voltammograms of (a) PDI-Cu/Cu and (b) PDI/Cu at different scan rate.

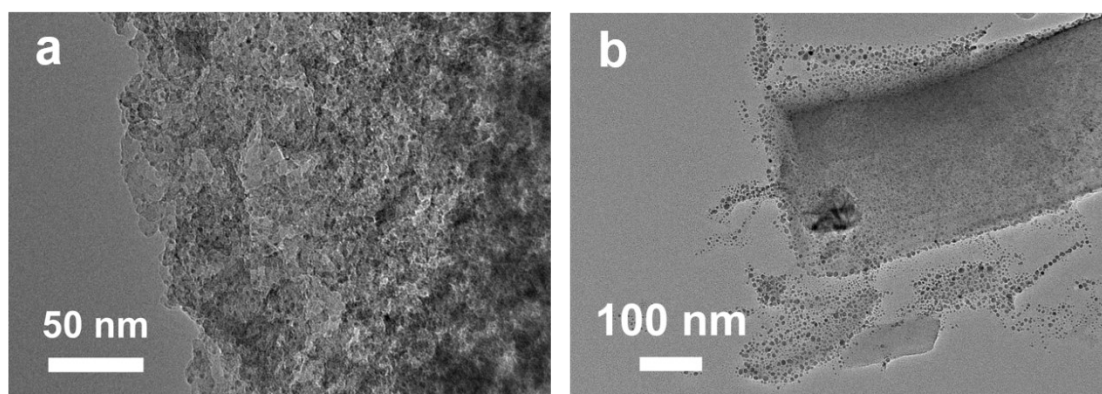


Figure S10. The TEM images of (a) PDI-Cu/Cu and (b) PDI/Cu after the electrochemical CO₂RR.

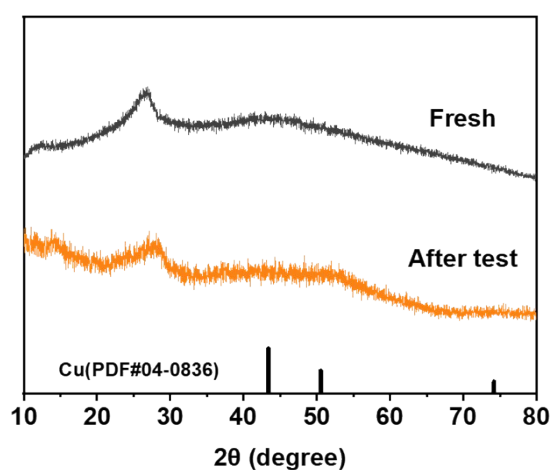


Figure S11. XRD patterns of before and after electrochemical CO₂RR of PDI-Cu.

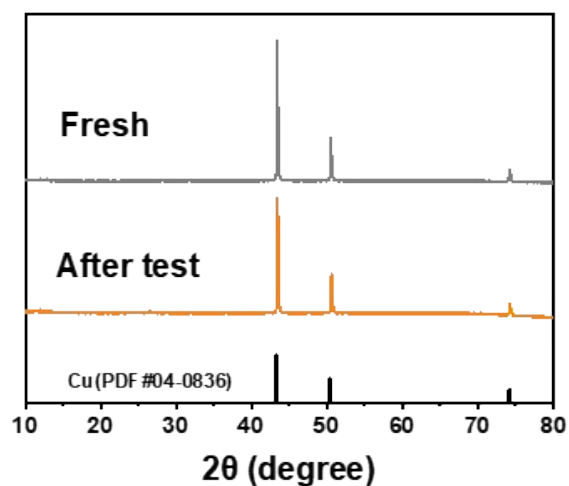


Figure S12. XRD patterns of before and after electrochemical CO₂RR of PDI-Cu/Cu.

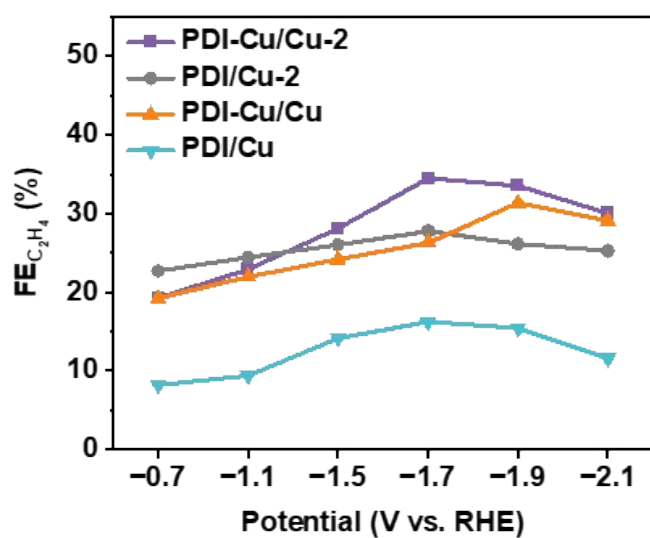


Figure S13. The FEs for C₂H₄ conversion catalyzed by PDI-Cu/Cu, PDI-Cu, PDI-Cu/Cu-2 and PDI/Cu-2.

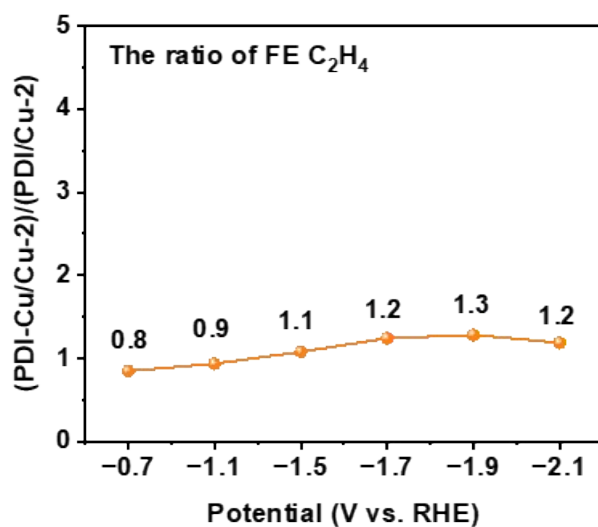


Figure S14. The FE (C_2H_4) ratio of PDI-Cu/Cu-2 to PDI/Cu-2.

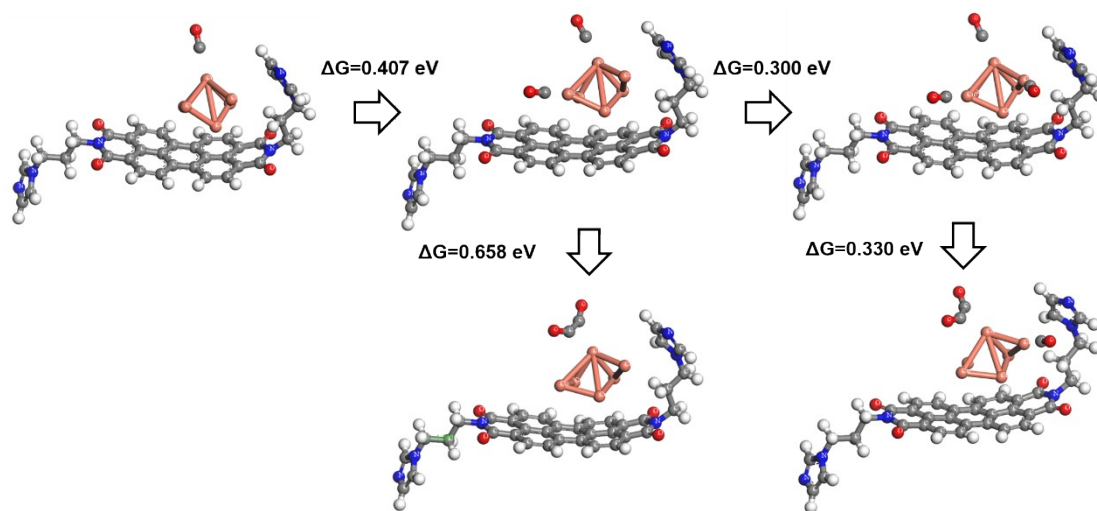


Figure S15. The complete structures of CO adsorption and C-C coupling on Cu clusters.

Table S1. The ICP results of the PDI-Cu, PDI-Cu/Cu and PDI/Cu samples.

	PDI-Cu	PDI-Cu/Cu	PDI/Cu
Content of Cu (wt%)	7.70	46.3	40.2

Table S2. The EXAFS curve-fitting results of the PDI-Cu samples.

Sample	Path	CN	R (Å)	σ^2 (10^{-3} Å²)
PDI-Cu	Cu-N	2.0(\pm 0.2)	1.95(\pm 0.01)	0.7(\pm 0.1)
	Cu-Cl	2.0(\pm 0.1)	2.30(\pm 0.02)	1.2(\pm 0.1)

Table S3. The ICP results of the PDI-Cu/Cu-2 and PDI/Cu-2 samples.

	PDI-Cu/Cu-2	PDI/Cu-2
Content of Cu (wt%)	74.7	84.2